CHARACTERIZATION AND OPTIMIZATION OF CPW ELECTRO-OPTIC MODULATORS FOR MICROWAVE AND MM-WAVE APPLICATIONS

G. Ghione, M. Goano, G. Omegna, M. Pirola
Dipartimento di Elettronica, Politecnico di Torino, Torino, Italy

S. Bosso, D. Frassati, A. Perasso
Pirelli Optical Systems, Milano, Italy

ABSTRACT

The paper presents a discussion on the experimental characterization and microwave modelling of coplanar electro-optic modulators on lithium niobate substrates. To introduce the issue, a discussion is presented on the design criteria for travelling-wave modulators. In particular, we show that attenuation is a main concern if modulation bandwidths in excess of 20 GHz are sought, while velocity matching can be achieved with comparative ease, as a survey of the available structures shows. Finally, the experimental characterization and modelling of some conventional modulator structures is presented, with the aim to assess their operating limits in terms of modulation bandwidth.

INTRODUCTION

Electro-optic modulators for the microwave and millimeter wave range are becoming increasingly important in high-speed optical communication systems. Despite the emergence of semiconductor amplitude modulators based on the field dependence of the material absorption, the best performances in terms of modulation bandwidth are still achieved by modulators based on piezoeletric materials, such as lithium niobate. From a system standpoint, wideband amplitude or phase modulators must satisfy two conflicting requirements: wide modulation bandwidth B and low driving voltage, often expressed through the parameter V_π, equal to the driving voltage required to achieve a π phase modulation. Although several solutions are available to achieve high operating frequency with narrow bandwidth, such as the use of periodic structures [1] or structures with phase reversal [2], extremely wide operating bandwidths can only be obtained through travelling wave modulators.

The frequency response of such devices (see Fig. 1, inset, for an example of travelling-wave amplitude Mach-Zehnder modulator) is controlled by a number of parameters. First of all, a flat response is only achieved if the line is impedance matched to the load and generator; impedance mismatch generates ripples in the electrical and electro-optic frequency response. Secondly, the modulator bandwidth mainly depends on two factors: the synchronous coupling of the RF and optical modes along the modulator, often described in terms of effective refractive index mismatch $\Delta n_{\text{eff}} = n_{\text{m}} - n_{\text{o}}$ between the effective indices of the microwave and optical modes, and the line attenuation α. Finally, the driving voltage should be low enough to ensure system compatibility, meaning that strong coupling has to be ensured between the microwave and optical fields.

During the last decade, travelling-wave lithium niobate modulators have undergone a continuous development with improvements in the modulation bandwidth from a few GHz to almost 100 GHz. This development has mainly concentrated on coplanar waveguide (CPW) RF electrode settings, coupled to diffused optical waveguides which, according to the kind of substrate (Z-cut or X-cut) were placed so as to couple with a vertical or horizontal component of the RF electric field, respectively. In order to obtain small values for V_π, the CPW gap was brought down to 10-15 μm. Taking into account that $n_{\text{o}} \approx 2.14$ [3] and that the CPW effective refractive index on $LiNbO_3$ substrate is $n_{\text{m}} \approx 3.5$, the natural mismatch between the CPW quasi-TEM mode and the optical mode is unacceptably high. In order to improve the velocity matching, a low-epsilon buffer layer is usually introduced below the electrodes, and the metal thickness is increased up to 15-30 μm. Other solutions include shield planes and oxide etching in the gaps, see Fig. 2 (d), (e), (g). The decrease in the microwave refractive index also enables to increase the line impedance up to the required 50 Ω level. Unfortunately, the use of very small lines increases the ohmic losses, and the V_π almost linearly increases with the buffer layer thickness. Taking into account that the products $V_\pi L$ and BL, where L is the modulator length, are almost constant for a given structure, it is clear that a trade-off has to be made between modulation bandwidth and driving voltage.

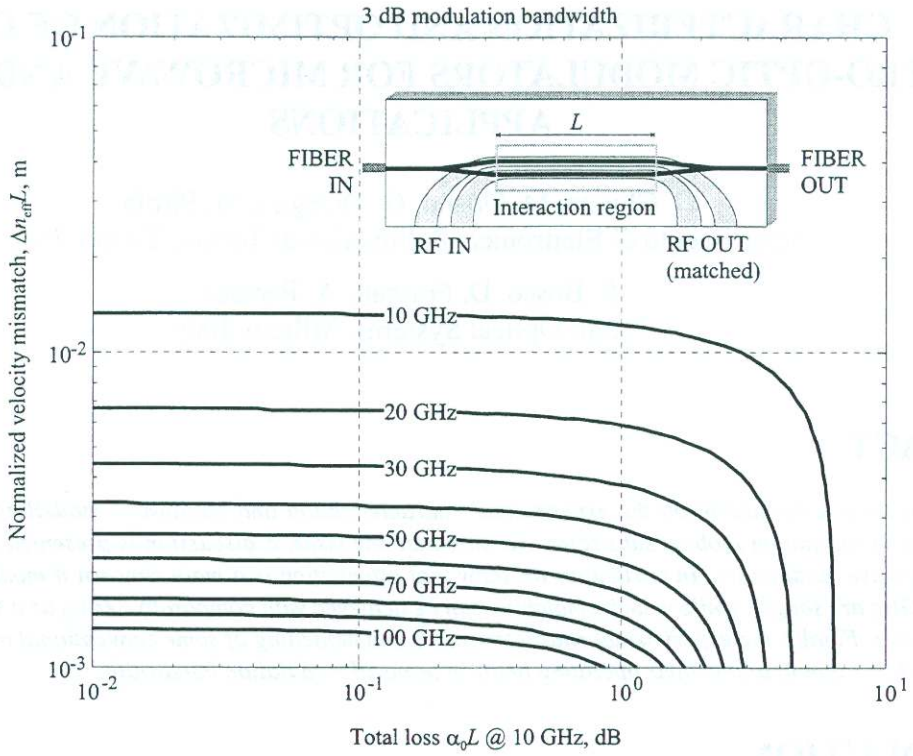

Figure 1: Constant optical bandwidth curves as a function of the total line attenuation (at 10 GHz) and of the normalized velocity mismatch.

BANDWIDTH REQUIREMENTS AND OPTIMIZATION

For a travelling-wave modulator, the requirement on bandwidth can be readily translated into a requirement on mismatch and attenuation. For the sake of simplicity, let us consider an impedance-matched modulator of length L. Straightforward transmission line analysis allows to express the normalized modulator response as [3]:

$$|m(f)| = \exp\left(-\frac{\alpha_0 L}{2}\sqrt{\frac{f}{f_0}}\right)\frac{\sinh u}{u} \tag{1}$$

where:

$$u = \frac{\alpha_0 L}{2}\sqrt{\frac{f}{f_0}} + \mathrm{j}\frac{\pi f}{c}\Delta n_{\mathrm{eff}} L. \tag{2}$$

The line attenuation α is expressed according to the skin-effect regime, as $\alpha = \alpha_0\sqrt{f/f_0}$ where f_0 is a reference frequency; c is the velocity of light in vacuo. The 3 dB optical modulation bandwidth is expressed such as $|m(B)|_{\mathrm{dB}} =$ -3 dB with respect to the low-frequency value. By computing B for several values of the total line loss $\alpha_0 L$ for a given frequency f_0 (assumed here as 10 GHz) and of the normalized mismatch $\Delta n_{\mathrm{eff}} L$, one obtains the result shown in Fig. 1 under the form of contour plot for B. From Fig. 1, one clearly sees that two regimes exist, wherein the bandwith is limited by mismatch (horizontal level curves) or by attenuation (vertical level curves). A rough estimate of the bandwidth achievable with a given structure is therefore:

$$B \approx \min(B_{\Delta n_{\mathrm{eff}}}, B_\alpha) \tag{3}$$

where $B_{\Delta n_{\mathrm{eff}}}$ is the mismatch-limited bandwidth, such as:

$$B_{\Delta n_{\mathrm{eff}}} L \approx \frac{0.134}{\Delta n_{\mathrm{eff}}} \quad \mathrm{GHz\ cm} \tag{4}$$

while B_α is the attenuation-limited bandwidth, such as:

$$\alpha(B_\alpha)L = \alpha_0 L\sqrt{\frac{B_\alpha}{f_0}} \approx 6.43 \quad \mathrm{dB}. \tag{5}$$

Cut	Z	Z	Z	Z	X	Z	Z	X	Z	Z	Z	Z
Ref.	[5]	[6]	[7]	[8]	[9]	[10]	[11]	[12]	[13]	[4]	[4]	[14]
Z_0, Ω	50	50	35	39	41	34	44	50	40	50	47	50
n_m	2.35	2.15		2.11	2.13	2.14	2.2	2.1	2.3	2.14	2.14	2.2
$B \cdot L$, GHz cm	40	48		160				142	40	100	80	90
$V_\pi \cdot L$, V cm	10.8	8.4		12.33				10.4	12.5	13	13.5	10
α @1 GHz, dB/cm	0.62							0.43	0.67	0.34	0.43	0.3

Table 1: Performances of the structures shown in Fig. 2.

For instance, to achieve 40 GHz bandwidth with $L = 4$ cm (cfr. [4, Sec.3]) one must have $\Delta n_{\text{eff}} = 0.08$ and $\alpha_0 \approx 0.25$ dB/cm at $f_0 = 1$ GHz (or equivalently 0.8 dB/cm at $f_0 = 10$ GHz).

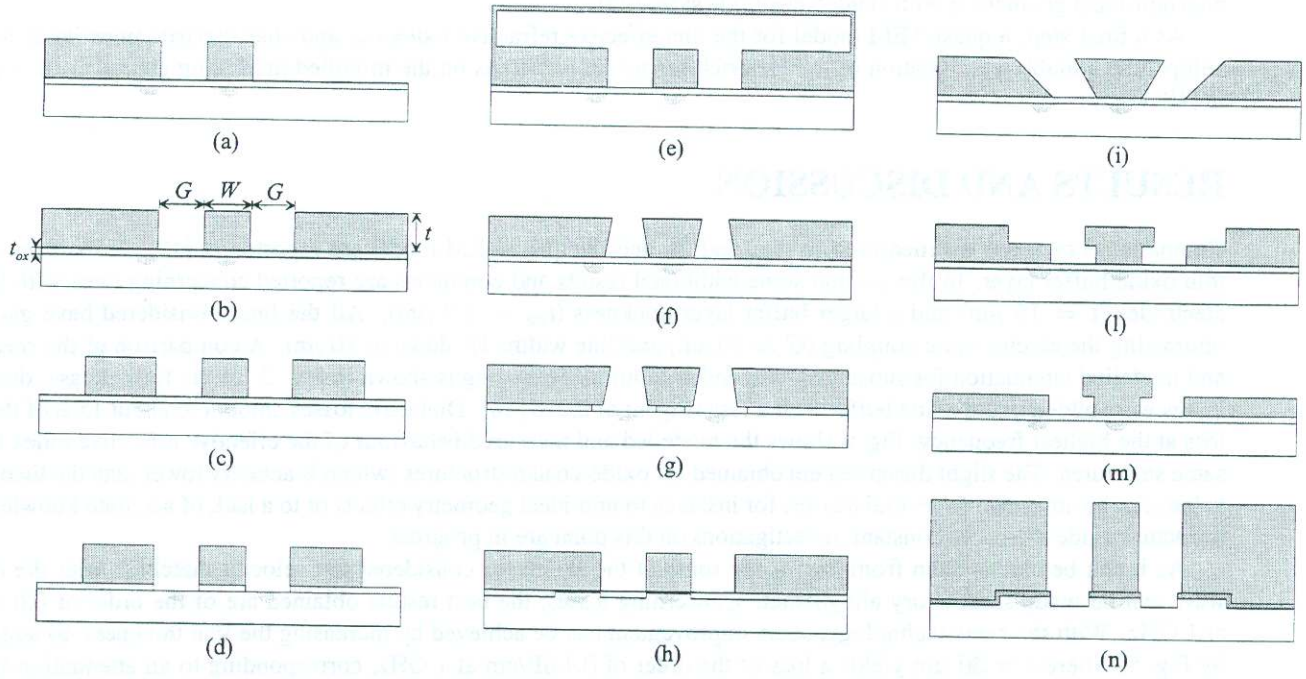

Figure 2: High-performance modulator structures on Z-cut and X-cut substrates. For line (f) the metallization angle is 10^o with respect to the vertical. Structures (i) and (l) are approximations to the real structure (m).

From the above discussion, it can be concluded that in the millimeter wave range the bandwidth limitation due to attenuation may become more significant than the limitation due to velocity mismatch. Concerning velocity mismatch, results from the literature show that many structures exist which ensure almost perfect matching, see Table 1.

Performance improvement has been less dramatic if we consider the line attenuation, see Tab. 1 and the data on the line losses of state-of-the art modulators reported in [15], Fig.8. Taking into account that, in the quasi-TEM approximation, $\alpha = \alpha_v n_m$ where α_v is the *in-vacuo* attenuation, reducing n_m to the optical value partly contributes to lower the line attenuation. Further improvements have been achieved by working with very thick electrodes; recently reported values at 1 GHz are $\alpha_0 = 0.43$ dB/cm for structure (b), $\alpha_0 = 0.34$ dB/cm at 1 GHz for structure (m) [4], and $\alpha_0 \approx 0.3$ dB/cm for structure (c) [16,17]. Although the conductor periphery, and therefore the losses, can be arbitrarily decreased by increasing the conductor thickness, electroplated conductors thicker than around 30 μm (see e.g. [16]) seem to be impossible to manufacture with the available technology. A different approach was followed in [4] where low-coupling electrodes where introduce to decrease losses, see Fig. 2 (i), (l), (m); however, improvements were not dramatic. Furthermore, actual losses can also exceed the conductor contribution, wherever dielectric losses in buffer layers arise, see [18] for a discussion.

In the present work, several test structures where manufactured on X-cut lithium niobate substrates with thickness $h = 1\,\text{mm}$ and $h = 500\,\mu\text{m}$. The transmission lines considered where of type (b) and (c), i.e. CPW with infinite or finite ground planes. Since the substrate is X-cut, the optical waveguides were placed in the middle of the slots. The oxide buffer layer was deposited through VPE with different thicknesses (0.5, 1, 1.5 μm) and the microwave electrodes were electroplated so as to achieve a thickness t comparable or larger than the slot width G, which is of the order of $10\,\mu\text{m}$ to optimize electro-optic coupling. For the sake of comparison, lines were also manufactured without oxide coating. Test structures also included tapers and launchers to allow for on-wafer probing. Further details can be found in [18].

The test structures were characterized through electrical measurements up to 40 GHz and the complex propagation constant $\gamma = \alpha + \mathrm{j}\beta$ was derived following the TRL approach [18–20]. Lines without oxide buffers showed a typical skin-effect frequency behaviour for the attenuation, while buffered lines also presented a detectable linear term in the attenuation, which could be attributed to dielectric losses associated to a loss angle of the order of 0.01.

The line impedance was finally extracted from γ following the approach in [21]; to this aim, the *in vacuo* line capacitance C_0 was exactly computed through a conformal mapping technique allowing for arbitrary line thickness [18] and also non-ideal geometries with slanted electrode sides [22].

As a final step, a quasi-TEM model for the line effective refractive index n_m and characteristic impedance was developed by suitable modification of the Heinrich model [23]. Details on the modified modelling approach are reported in [18].

RESULTS AND DISCUSSION

Comparisons between the measured α, n_m, and Z_0 and the quasi-TEM model are reported in [18, 22] for lines with a thin oxide buffer layer. In this section some additional results and comments are reported concerning lines with thicker electrodes ($t = 15\ \mu\text{m}$) and a larger buffer layer thickness ($t_{ox} = 1.2\ \mu\text{m}$). All the lines considered have gap sizes optimizing the electro-optic coupling ($G \approx 10\,\mu\text{m}$) and line widths W down to $10\ \mu\text{m}$. A comparison of the measured and modelled attenuation for substrates with and without oxide coating is shown in Fig. 3. In the former case, dielectric losses were added in the oxide buffer with a loss tangent of 0.016 [18]. Dielectric losses amount to about 15% of the total loss at the highest frequency. Fig. 4 shows the modelled and measured behaviour of the effective refractive index for the same structures. The slight disagreement obtained for oxide-coated structures (which is actually lower than the theoretical value) can be attributed to several causes, for instance to non-ideal geometry effects or to a lack of accurate knowledge of the actual oxide dielectric constant; investigations on this point are in progress.

As it can be clearly seen from Fig. 4, for some of the structures considered the velocity matching with the optical wave can be made satisfactory altoghether. Concerning losses, the best results obtained are of the order of 0.6 dB/cm at 1 GHz. With the same technology, some improvement can be achieved by increasing the line thickness, as suggested by Fig. 5, where $t = 30\ \mu\text{m}$ yields a loss of the order of 0.4 dB/cm at 1 GHz, corresponding to an attenuation-limited optical bandwidth of $256/L^2$ Ghz where L is the modulator length in cm. Larger values of t, besides being outside the technological range, yield a minor improvement only. An additional decrease of the line loss can be obtained by increasing G at the expense of the driving voltage; in fact the value reported in [17] of 0.27 dB/cm at 1 GHz was obtained width a $25\ \mu\text{m}$ gap.

ACKNOWLEDGEMENTS

This research was partially supported by CNR (National Council of Research) through the MADESS II project.

References

[1] J. H. Schaffner and R. R. Hayes, "Velocity-matching in millimeter wave integrated optic modulators with periodic electrodes," *J. Lightwave Technol.*, vol. LT-12, no. 3, pp. 503–511, Mar. 1994.

[2] K. W. Hui, K. S. Chiang, B. Y. Wu, and Z. H. Zhang, "Electrode optimization for high-speed traveling-wave integrated optic modulator," *J. Lightwave Technol.*, vol. LT-16, no. 2, pp. 232–238, Feb. 1998.

[3] R. C. Alferness, "Waveguide electrooptic modulators," *IEEE Trans. Microwave Theory Tech.*, vol. MTT-30, no. 8, pp. 1121–1137, Aug. 1982.

[4] R. Madabhushi, "Microwave attenuation reduction techniques for wide-band Ti:$LiNbO_3$ optical modulators," *IEICE Trans. Electron.*, vol. E81-C, no. 8, pp. 1321–1327, Aug. 1998.

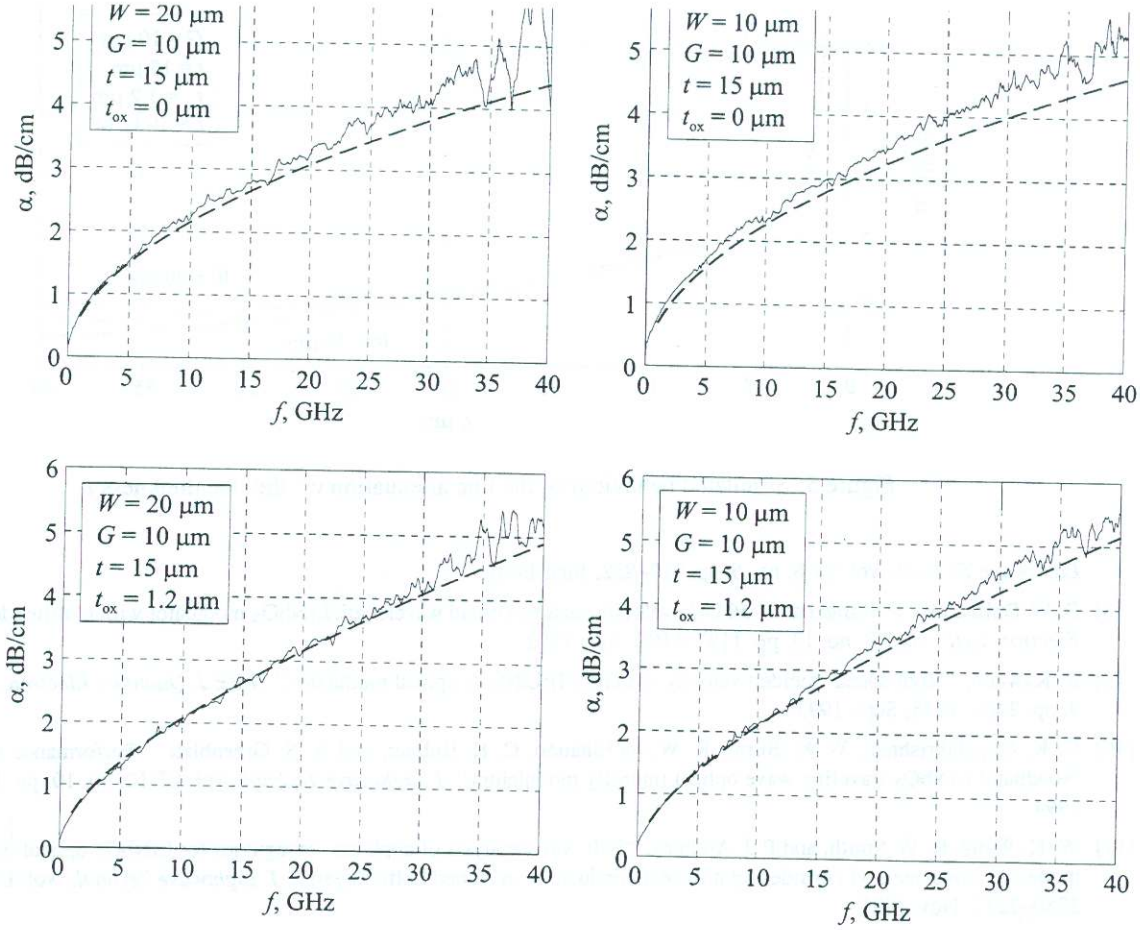

Figure 3: Measured (continuous line) and modelled (dashed line) frequency behaviour of the attenuation of lines with and without oxide buffer layer.

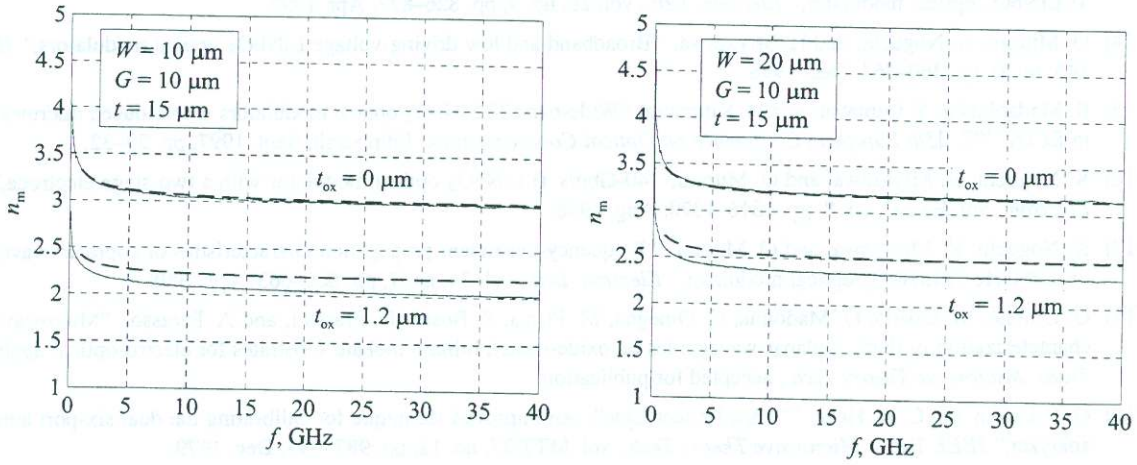

Figure 4: Measured (continuous line) and modelled (dashed line) frequency behaviour of the effective refractive index of lines with and without oxide buffer layer.

[5] M. Seino, N. Mekada, T. Yamane, Y. Kubota, M. Doi, and T. Nakazawa, "20-GHz 3 dB-bandwidth Ti:$LiNbO_3$ Mach-Zehnder modulator," in *ECOC '90*, Amsterdam, Sept. 1990, pp. 999–1002.

[6] X. Zhang and T. Miyoshi, "Optimum design of coplanar waveguide for $LiNbO_3$ optical modulator," *IEEE Trans. Microwave Theory Tech.*, vol. MTT-43, no. 3, pp. 523–528, Mar. 1995.

[7] J. C. Yi, S. H. Kim, and S. S. Choi, "Finite-element method for the impedance analysis of traveling-wave modulators," *J.*

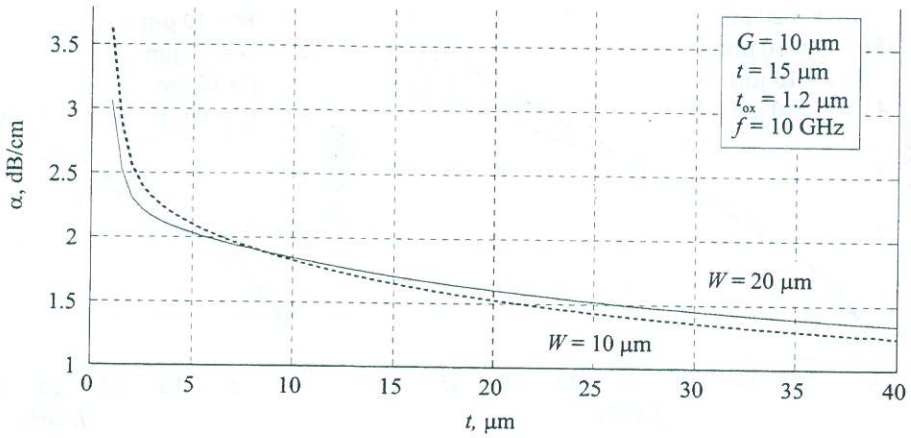

Figure 5: Simulated behaviour of the line attenuation *vs.* the line thickness t.

Lightwave Technol., vol. LT-8, no. 6, pp. 817–822, June 1990.

[8] D. W. Dolfi and T. R. Ranganath, "50 GHz velocity-matched broad wavelength $LiNbO_3$ modulator with multimode active section," *Electron. Lett.*, vol. 28, no. 13, pp. 1197–1198, June 1992.

[9] K. Kawano, "High-speed shielded velocity-matched Ti:$LiNbO_3$ optical modulator," *IEEE J. Quantum Electron.*, vol. QE-29, no. 9, pp. 2466–2475, Sept. 1993.

[10] G. K. Gopalakrishnan, W. K. Burns, R. W. McElhanon, C. H. Bulmer, and A. S. Greenblatt, "Performance and modeling of broadband $LiNbO_3$ traveling wave optical intensity modulators," *J. Lightwave Technol.*, vol. LT-12, no. 10, pp. 1807–1819, Oct. 1994.

[11] W.-K. Wang, R. W. Smith, and P. J. Anthony, "Full-wave analysis of coplanar waveguides for $LiNbO_3$ optical modulators by the mode-matching method considering nonideal conductors on etched buffer layers," *J. Lightwave Technol.*, vol. LT-13, no. 11, pp. 2250–2257, Nov. 1995.

[12] O. Mitomi, K. Noguchi, and H. Miyazawa, "Design of ultra-broad-band $LiNbO_3$ optical modulator with ridge structure," *IEEE Trans. Microwave Theory Tech.*, vol. MTT-43, no. 9, pp. 2203–2207, Sept. 1995.

[13] G. K. Gopalakrishnan, C. H. Bulmer, W. K. Burns, R. W. McElhanon, and A. S. Greenblatt, "40 GHz, low half-wave voltage Ti:$LiNbO_3$ optical modulator," *Electron. Lett.*, vol. 28, no. 9, pp. 826–827, Apr. 1992.

[14] O. Mitomi, K. Noguchi, and H. Miyazawa, "Broadband and low driving-voltage $LiNbO_3$ optical modulators," *IEE Proc.-J*, vol. 145, no. 6, pp. 360–364, Dec. 1998.

[15] R. Madabhushi, Y. Uematsu, and M. Kitamura, "Wide-band Ti:$LiNbO_3$ optical modulators with reduced microwave attenuation," in *ECOC '97. 23th European Conference on Optical Communication*, Edinburgh, Sept. 1997, pp. 29–32.

[16] K. Noguchi, H. Miyazawa, and O. Mitomi, "40-Gbit/s Ti:$LiNbO_3$ optical modulator with a two-stage electrode," *IEICE Trans. Electron.*, vol. E81-C, no. 8, pp. 1316–1320, Aug. 1998.

[17] K. Noguchi, H. Miyazawa, and O. Mitomi, "Frequency-dependent propagation characteristics of coplanar waveguide electrode on 100 GHz Ti:$LiNbO_3$ optical modulator," *Electron. Lett.*, vol. 34, no. 7, pp. 661–663, Apr. 1998.

[18] G. Ghione, M. Goano, G. Madonna, G. Omegna, M. Pirola, S. Bosso, D. Frassati, and A. Perasso, "Microwave modeling and characterization of thick coplanar waveguides on oxide-coated lithium niobate substrates for electro-optical applications," *IEEE Trans. Microwave Theory Tech.*, accepted for publication.

[19] G. F. Engen and C. A. Hoer, ""Thru-Reflect-Line": An improved technique for calibrating the dual six-port automatic network analyzer," *IEEE Trans. Microwave Theory Tech.*, vol. MTT-27, no. 12, pp. 987–993, Dec. 1979.

[20] R. B. Marks, "A multiline method of network analyzer calibration," *IEEE Trans. Microwave Theory Tech.*, vol. MTT-39, no. 7, pp. 1205–1215, July 1991.

[21] R. B. Marks and D. F. Williams, "Characteristic impedance determination using propagation constant measurement," *IEEE Microwave Guided Wave Lett.*, vol. 1, no. 6, pp. 141–143, June 1991.

[22] G. Ghione, M. Goano, and M. Pirola, "Exact, conformal-mapping models for the high-frequency losses of coplanar waveguides with thick electrodes of rectangular or trapezoidal cross section," in *IEEE MTT-S International Microwave Symposium*, Anaheim, CA, June 1999, vol. 4, pp. 1311–1314.

[23] W. Heinrich, "Quasi-TEM description of MMIC coplanar lines including conductor-loss effects," *IEEE Trans. Microwave Theory Tech.*, vol. MTT-41, no. 1, pp. 45–52, Jan. 1993.